

# Detection of the Number of Paths over Wireless Channels: A Maximum Likelihood Approach

Souheib Ben Amor<sup>†</sup>, Sofiène Affes<sup>†</sup>, and Ali Ghrayeb<sup>‡</sup>

<sup>†</sup>INRS-EMT, Université du Québec, Montréal, QC, Canada, Emails: {souheib.ben.amor, affes}@emt.inrs.ca

<sup>‡</sup>Texas A&M University at Qatar, Doha, Qatar, Email: ali.ghrayeb@qatar.tamu.edu

**Abstract**—In this paper, we tackle the problem of Multipath detection for joint angle and delay estimation (JADE) purposes. By exploiting the sparsity feature of a carefully designed pseudo-pdf, we propose a novel approach that enables the accurate estimation of the unknown number of paths over a wide range of practical signal-to-noise ratios (SNRs). Computer simulations show the distinct advantage of the new solution over state-of-the-art techniques in terms of accuracy. Most remarkably, they suggest that the proposed technique provide accurate estimates even when the number of paths exceeds the antenna size.

**Index Terms**—JADE, signal detection, maximum likelihood, importance sampling, antenna arrays.

## I. INTRODUCTION

In parametric multipath propagation models, a source signal impinges on an antenna array through a number of rays, each described by an angle-of-arrival (AoA), a time delay (TD), and a path gain. The joint angle and delay estimation (JADE) problem consists then in jointly estimating all the AoAs and their corresponding TDs from a finite number of received samples. The JADE problem arises in many practical situations ranging from military applications (e.g., radar and sonar) to broadband wireless communication systems.

Typically, the power to characterize each path with its own angle and delay endows the system with stronger sensorial capabilities leading, for instance, to more robust beamforming techniques [2] and enhanced equalization performance [3]. In comparison with disjoint estimation techniques which first estimate the delays and then the corresponding angles, the joint estimation of these space-time parameters (i.e., JADE) is more accurate in cases where multiple rays have nearly equal delays or angles [2]. Moreover, contrarily to JADE, the number of estimated angles in direction of arrival (DOA) only estimation must be smaller than the number of antennae. Thus DOA-only estimators would require large-size antenna arrays in highly dense multipath environments.

A number of JADE techniques have been reported in the literature [4-8]. All the proposed solutions requires that the number of paths to be known. This information is usually unavailable in real-life scenarios and needs to be estimated. One solution is to use a method for detecting the number of signals such as Akaike's information criterion (AIC) [9], minimum description length (MDL) [10], and the eigenvalue

This work was made possible by NPRP grant NPRP 5-250-2-087 from the Qatar National Research Fund (a member of Qatar Foundation). The statements made herein are solely the responsibility of the authors. Work published in part in a journal version [1].

forms of AIC and MDL [11]. However, these techniques are unable to provide estimates when the number of paths exceeds the number of antennas elements.

In this paper, we propose a new technique for detection of the number of paths. It builds upon a very accurate approximation of the true compressed likelihood function (CLF). In fact, by exploiting the sparsity of the proposed pseudo-pdf, the new approach is able to estimate accurately the number of paths.

We organize the rest of this paper as follows: In section II, we introduce the system model that will be used throughout the article. In section III, we derive the CLF of the system. In section IV, we develop the new approach for the estimation of the number of paths. In section V, we assess the performance of the new approach and benchmark it against both AIC and MDL techniques. Finally, we draw out some concluding remarks in section VI.

We define beforehand some of the common notations that will be adopted in this paper. Vectors and matrices are represented in lower- and upper-case bold fonts, respectively.  $\{\cdot\}^T$  and  $\{\cdot\}^H$  denote the conjugate and Hermitian (i.e., transpose conjugate) operators and  $\det\{\cdot\}$  returns the determinant of any square matrix. The Euclidean norm of any vector is denoted as  $\|\cdot\|$  and  $\mathbf{I}_N$  denotes the  $(N \times N)$  identity matrix. For any matrix  $\mathbf{X}$ ,  $[\mathbf{X}]_q$  and  $[\mathbf{X}]_{l,k}$  denote its  $q^{th}$  column and  $(l, k)^{th}$  entry, respectively. The kronecker product of any two matrices  $\mathbf{X}$  and  $\mathbf{Y}$  is denoted as  $\mathbf{X} \otimes \mathbf{Y}$ . In addition,  $\{\cdot\}^*$ ,  $\angle\{\cdot\}$ , and  $|\cdot|$  return the conjugate, modulus, and angle of any complex number, respectively. Finally,  $\mathbb{E}\{\cdot\}$  stands for the statistical expectation,  $j$  is the pure complex number that verifies  $j^2 = -1$ , and the notation  $\triangleq$  is used for definitions.

## II. SYSTEM MODEL

Consider an antenna array consisting of  $P$  antenna elements immersed in a homogeneous medium in the far field of one source that is transmitting a planar wave. The transmitted signal undergoes multiple reflections and impinges on the antenna array from  $\bar{Q}$  different angles  $(\bar{\alpha}_1, \bar{\alpha}_2, \dots, \bar{\alpha}_{\bar{Q}})$  with associated time delays  $(\bar{\tau}_1, \bar{\tau}_2, \dots, \bar{\tau}_{\bar{Q}}) \subset [0, \tau_{\max}]^{\bar{Q}}$  where  $\tau_{\max}$  can be as large as desired. Note here that we use the overbar symbol to distinguish the true AoAs and TDs,  $\{\bar{\alpha}_q\}_q$  and  $\{\bar{\tau}_q\}_q$ , from the unknown generic<sup>1</sup> ones,  $\{\alpha_q\}_q$  and  $\{\tau_q\}_q$ .

<sup>1</sup>For the same reasons, we use  $\bar{Q}$  to denote the true unknown number of paths that will be estimated later in Section IV.

By assuming ideal frequency synchronization, the continuous-time received signal at the  $p^{\text{th}}$  antenna,  $p = 1, 2, \dots, P$ , can be modeled as follows:

$$x_p(t) = \sum_{q=1}^{\bar{Q}} \bar{\gamma}_q s(t - \bar{\tau}_q) e^{j\pi\varphi_p(\bar{\alpha}_q)} + w_p(t), \quad (1)$$

where  $\{\bar{\gamma}_q\}_{q=1}^{\bar{Q}}$  are the true complex path gains which are assumed to be unknown as well and  $\{\varphi_p(\alpha)\}_{p=1}^P$  are some real-valued angular transformations that depend on the geometry of the planar array configuration. Typically, uniform linear arrays (ULAs) and uniform circular arrays (UCAs) remain by far the most studied cases in the open literature. For these two popular configurations, the angular transformations are given by:

$$\varphi_p(\alpha) = \begin{cases} (p-1) \sin(\alpha), & \text{(ULA)} \\ \frac{\cos(\alpha - 2[p-1]\pi/P)}{2 \sin(\pi/P)}. & \text{(UCA)} \end{cases}$$

The noise components,  $w_p(t)$ , are assumed to be spatially and temporally white and modeled by zero-mean complex Gaussian random processes with independent real and imaginary parts each of variance  $\sigma^2/2$ . The known transmitted signal,  $s(t)$ , is a linear chirp signal which is generally expressed as  $s(t) = A \sin(2\pi[f_0 + vt]t)$ . Here,  $A$  is the amplitude and  $v = \frac{f_{\max} - f_0}{t_{\max}}$  with  $f_0$  and  $f_{\max}$  being, respectively, the minimum and maximum frequencies of the chirp attained at time instants  $t_0 = 0$  and  $t_{\max}$  which define the boundaries of the observation window  $[0, t_{\max}]$ . After sampling the continuous-time received signal in (1) at time instants  $\{t_m = mT_s\}_{m=0}^{M-1}$ , with sampling period  $T_s$ , one obtains the following  $M$  samples over each  $\{p^{\text{th}}\}_{p=1}^P$  antenna:

$$x_p(t_m) = \sum_{q=1}^{\bar{Q}} \bar{\gamma}_q s(t_m - \bar{\tau}_q) e^{j\pi\varphi_p(\bar{\alpha}_q)} + w_p(t_m), \quad (2)$$

with  $m = 0, 2, \dots, M-1$ . For mathematical convenience, we group all the unknown multipath parameters in the following three vectors:  $\bar{\alpha} = [\bar{\alpha}_1, \bar{\alpha}_2, \dots, \bar{\alpha}_{\bar{Q}}]^T$ ,  $\bar{\tau} = [\bar{\tau}_1, \bar{\tau}_2, \dots, \bar{\tau}_{\bar{Q}}]^T$ , and  $\bar{\gamma} = [\bar{\gamma}_1, \bar{\gamma}_2, \dots, \bar{\gamma}_{\bar{Q}}]^T$ . We further gather the samples collected across all the antenna elements at each  $m^{\text{th}}$  time index (known as *snapshot* in array signal processing terminology) into a single vector,  $\mathbf{x}(t_m) = [x_1(t_m), x_2(t_m), \dots, x_P(t_m)]^T$ , given by:

$$\mathbf{x}(t_m) = \sum_{q=1}^{\bar{Q}} \mathbf{a}(\bar{\alpha}_q) \bar{\gamma}_q s(t_m - \bar{\tau}_q) + \mathbf{w}(t_m), \quad (3)$$

where  $\mathbf{w}(t_m) = [w_1(t_m), w_2(t_m), \dots, w_P(t_m)]^T$  is the corresponding noise vector and:

$$\mathbf{a}(\alpha) \triangleq [e^{j\pi\varphi_1(\alpha)}, e^{j\pi\varphi_2(\alpha)}, \dots, e^{j\pi\varphi_P(\alpha)}]^T, \quad (4)$$

is the array *steering vector* defined for any direction  $\alpha$ . Our goal in the remainder of this paper is to estimate the parameter  $\bar{Q}$  given the  $M$  snapshots  $\{\mathbf{x}(t_m)\}_{m=0}^{M-1}$ .

### III. DERIVATION OF THE COMPRESSED LIKELIHOOD FUNCTION (CLF)

In this section, we will derive the CLF that depends on the parameters of interest only [12], namely  $\bar{\tau}$ ,  $\bar{\alpha}$ . In fact, since  $\mathbf{w}(m) \sim \mathcal{N}(\mathbf{0}, \sigma^2 \mathbf{I}_P)$ , it can be shown that the actual log-likelihood function (LLF) (after dropping the constant terms) is given by where:

$$\mathcal{L}(\alpha, \tau, \gamma) = \sum_{m=1}^M \left\| \mathbf{x}(t_m) - \sum_{q=1}^{\bar{Q}} \gamma_q \mathbf{a}(\alpha_q) s(t_m - \tau_q) \right\|^2. \quad (5)$$

Furthermore, owing to the Parseval's identity, it follows that  $\mathcal{L}(\alpha, \tau, \gamma)$  can be alternatively expressed in the frequency domain as follows:

$$\mathcal{L}(\alpha, \tau, \gamma) \approx \sum_{m=1}^M \left\| \mathbf{x}(\omega_m) - \sum_{q=1}^{\bar{Q}} \gamma_q \mathbf{a}(\alpha_q) e^{-j\omega_m \tau_q} s(\omega_m) \right\|^2, \quad (6)$$

where  $\{\omega_m = \frac{m-1}{MT_s}\}_{m=1}^M$  is the  $m^{\text{th}}$  frequency bin and  $\{\mathbf{x}(\omega_m)\}_m$  and  $\{s(\omega_m)\}_m$  are the DFTs of  $\{\mathbf{x}(t_m)\}_m$  and  $\{s(t_m)\}_m$ , respectively, with the approximation stemming from the fact that  $\{\tau_q\}_{q=1}^{\bar{Q}}$  are not necessarily integer multiples of the sampling period  $T_s$ . Now let  $\mathbf{A}(\alpha)$  denote the array *steering matrix* that is defined for any  $\alpha = [\alpha_1, \alpha_2, \dots, \alpha_{\bar{Q}}]^T$  as follows:

$$\mathbf{A}(\alpha) \triangleq [\mathbf{a}(\alpha_1) \mathbf{a}(\alpha_2) \dots \mathbf{a}(\alpha_{\bar{Q}})], \quad (7)$$

in which  $\mathbf{a}(\alpha)$  is the steering vector given in (4). Then, by defining the following  $(\bar{Q} \times \bar{Q})$  diagonal matrix:

$$\Phi_m(\tau) \triangleq s(\omega_m) \text{diag}(e^{-j\omega_m \tau_1}, e^{-j\omega_m \tau_2}, \dots, e^{-j\omega_m \tau_{\bar{Q}}}), \quad (8)$$

for  $m = 1, 2, \dots, M$ , it can be shown that (6) is equivalent to:

$$\begin{aligned} \mathcal{L}(\alpha, \tau, \gamma) &\approx \sum_{m=1}^M \left\| \mathbf{x}(\omega_m) - s(\omega_m) \mathbf{A}(\alpha) \Phi_m(\tau) \gamma \right\|^2 \\ &= \left\| \mathbf{x} - [\mathbf{I}_M \otimes \mathbf{A}(\alpha)] \Phi(\tau) \gamma \right\|^2, \end{aligned} \quad (9)$$

where  $\mathbf{x} = [\mathbf{x}(\omega_1)^T \mathbf{x}(\omega_2)^T \dots \mathbf{x}(\omega_M)^T]^T$ ,  $\otimes$  denotes the Kronecker product, and  $\Phi(\tau)$  is the following  $(M\bar{Q} \times \bar{Q})$  matrix:

$$\Phi(\tau) = [\Phi_1(\tau)^T \Phi_2(\tau)^T \dots \Phi_M(\tau)^T]^T. \quad (10)$$

Yet, significant computational savings follow from the use of least square (LS) to obtain the channel gains estimates:

$$\hat{\gamma}_{\text{MLE}} = \underbrace{[\mathbf{I}_M \otimes \mathbf{A}(\alpha)] \Phi(\tau)}_{\triangleq \mathbf{D}}^\dagger \mathbf{x}, \quad (11)$$

where  $\mathbf{D}^\dagger$  is the Moore-Penrose pseudo-inverse of  $\mathbf{D}$  given by  $\mathbf{D}^\dagger = (\mathbf{D}^H \mathbf{D})^{-1} \mathbf{D}$ . Now, by substituting  $\hat{\gamma}_{\text{MLE}}$  for  $\gamma$  in (9) and after some straightforward algebraic manipulations,

we obtain as an objective function the so-called CLF which depends solely on  $\alpha$  and  $\tau$ :

$$\mathcal{L}_c(\alpha, \tau) = \mathbf{x}^H \mathbf{D} (\mathbf{D}^H \mathbf{D})^{-1} \mathbf{D}^H \mathbf{x}. \quad (12)$$

By revisiting (12), one can easily recognize that the original CLF cannot be directly expressed as a separable function due to the presence of the matrix inverse  $(\mathbf{D}^H \mathbf{D})^{-1}$ . Fortunately, we show in the sequel that  $\mathbf{D}^H \mathbf{D}$  can be accurately approximated by a diagonal matrix. In fact, by recalling the expression of  $\mathbf{D}$  in (11) and using some basic properties of the Kronecker product, it follows that:

$$\begin{aligned} \mathbf{D}^H \mathbf{D} &= \Phi(\tau)^H [\mathbf{I}_M \otimes \mathbf{A}(\alpha)^H] [\mathbf{I}_M \otimes \mathbf{A}(\alpha)] \Phi(\tau), \\ &= \Phi(\tau)^H \left( \mathbf{I}_M \otimes [\mathbf{A}(\alpha)^H \mathbf{A}(\alpha)] \right) \Phi(\tau). \end{aligned} \quad (13)$$

Then, by noticing that  $\mathbf{I}_M \otimes [\mathbf{A}(\alpha)^H \mathbf{A}(\alpha)]$  is a block-diagonal matrix, it can be shown that:

$$\mathbf{D}^H \mathbf{D} = \sum_{m=1}^M \Phi_m(\tau)^H \mathbf{A}(\alpha)^H \mathbf{A}(\alpha) \Phi_m(\tau). \quad (14)$$

Next, by recalling from (7) and (8) that the  $l^{\text{th}}$  column of the steering matrix is  $[\mathbf{A}(\alpha)]_l = \mathbf{a}(\alpha_l)$  and that  $\Phi_m(\tau)$  is a diagonal matrix, we immediately have  $[\mathbf{A}(\alpha) \Phi_m(\tau)]_l = [\Phi_m(\tau)]_{l,l} [\mathbf{A}(\alpha)]_l = s(\omega_m) e^{-j\omega_m \tau_l} \mathbf{a}(\alpha_l)$ . The  $(l, k)^{\text{th}}$  entry of  $\mathbf{D}^H \mathbf{D}$  is thus obtained as:

$$[\mathbf{D}^H \mathbf{D}]_{l,k} = \left( \sum_{m=1}^M |s(\omega_m)|^2 e^{j\omega_m(\tau_l - \tau_k)} \right) \times \left( \sum_{p=1}^P e^{j\pi(p-1)[\cos(\alpha_k) - \cos(\alpha_l)]} \right). \quad (15)$$

In particular, the diagonal elements obtained by setting  $k = l$  in (15) all have the same following expression:

$$[\mathbf{D}^H \mathbf{D}]_{k,k} = P \sum_{m=1}^M |s(\omega_m)|^2. \quad (16)$$

Due to the destructive superposition (for  $l \neq k$ ) of the complex exponentials<sup>2</sup> in (15), one could expect the off-diagonal entries of  $\mathbf{D}^H \mathbf{D}$  to be very small compared to its diagonal ones thereby allowing the following much useful approximation:

$$\mathbf{D}^H \mathbf{D} \approx P E_s \mathbf{I}_{\bar{Q}}, \quad (17)$$

where  $E_s = \sum_{m=1}^M |s(\omega_m)|^2$  is the energy of the transmitted signal. To corroborate our claim, we define the ratio of the off-diagonal over diagonal entries of the matrix  $\mathbf{D}^H \mathbf{D}$  as follows:

$$\beta_{l,k} \triangleq \frac{\left( \sum_{m=1}^M |s(\omega_m)|^2 e^{j\omega_m(\tau_l - \tau_k)} \right) \left( \sum_{p=1}^P e^{j\pi(p-1)\pi(\cos(\alpha_k) - \cos(\alpha_l))} \right)}{P \sum_{m=1}^M |s(\omega_m)|^2}, \quad (18)$$

<sup>2</sup>This is reminiscent of multipath fading in wireless channels.

then generate a very large number of couples  $(\tau_l, \tau_k)$  and  $(\alpha_l, \alpha_k)$  uniformly distributed in  $[0, \tau_{\max}]^2$  and  $[0, \pi]^2$ . After injecting these realizations into (18), we compute and plot in Fig. 1 the complementary cumulative distribution function (CCDF) of  $|\beta_{l,k}|$ , i.e.,  $F_c(x) = Pr[|\beta_{l,k}| \geq x]$ .

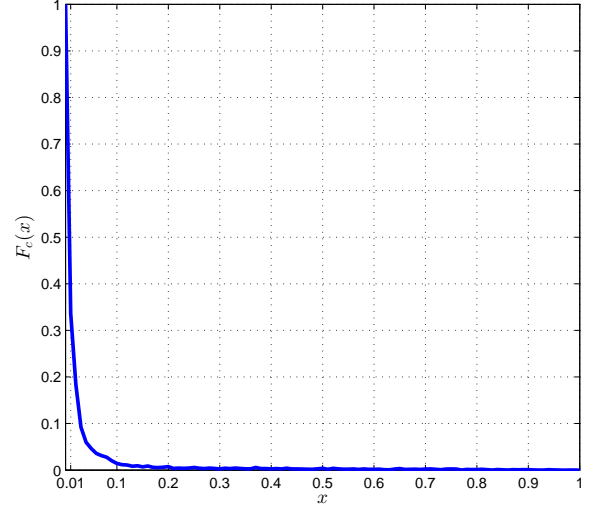


Figure 1. CCDF of the magnitude of the ratio between the off-diagonal and diagonal entries of the matrix  $\mathbf{D}^H \mathbf{D}$ .

Clearly, Fig. 1 suggests that the off-diagonal elements of  $\mathbf{D}^H \mathbf{D}$  can indeed be neglected compared to its diagonal ones since  $|\beta_{l,k}|$  has an almost-zero probability to exceed 0.1 for all  $l \neq k$ . Therefore, (17) is a valid and accurate approximation for  $\mathbf{D}^H \mathbf{D}$  which is used in (12) to obtain the following accurate approximation for the CLF:

$$\mathcal{L}_c(\alpha, \tau) \approx \frac{1}{P E_s} \mathbf{x}^H \mathbf{D} \mathbf{D}^H \mathbf{x}. \quad (19)$$

Then, by recalling from (11) that  $\mathbf{D} = [\mathbf{I}_M \otimes \mathbf{A}(\alpha)] \Phi(\tau)$ , it follows from (19) that:

$$\mathcal{L}_c(\alpha, \tau) = \frac{1}{P E_s} \|\Phi(\tau)^H [\mathbf{I}_M \otimes \mathbf{A}(\alpha)^H] \mathbf{x}\|^2. \quad (20)$$

Now, by recalling that  $\mathbf{x} = [\mathbf{x}(\omega_1)^T \mathbf{x}(\omega_2)^T \dots \mathbf{x}(\omega_M)^T]^T$  and using (10) it can be shown that:

$$\Phi(\tau)^H [\mathbf{I}_M \otimes \mathbf{A}(\alpha)^H] \mathbf{x} = \sum_{m=1}^M (\mathbf{A}(\alpha) \Phi_m(\tau))^H \mathbf{x}(\omega_m).$$

Therefore, it follows from (20) that:

$$\mathcal{L}_c(\alpha, \tau) \approx \frac{1}{P E_s} \sum_{q=1}^{\bar{Q}} \left| \sum_{m=1}^M [\mathbf{A}(\alpha) \Phi_m(\tau)]_q^H \mathbf{x}(\omega_m) \right|^2.$$

After some straightforward algebraic manipulations, we obtain the following much useful approximation for the CLF:

$$\mathcal{L}_c(\alpha, \tau) \approx \frac{1}{P E_s} \sum_{q=1}^{\bar{Q}} I(\alpha_q, \tau_q), \quad (21)$$

in which  $I(\alpha, \tau)$  is the periodogram of the signal given by:

$$I(\alpha, \tau) = \left| \sum_{p=1}^P e^{j\pi(p-1)\cos(\alpha)} \sum_{m=1}^M s(\omega_m) x_p^*(\omega_m) e^{-j2\pi\tau\omega_m} \right|^2, \quad (22)$$

where  $x_p(\omega_m)$  is the  $p^{\text{th}}$  element of the vector  $\mathbf{x}(\omega_m)$ . Owing to the decomposition of the *approximate* CLF in (21) as the superposition of the separate contributions pertaining to the  $\bar{Q}$  angle-delay pairs, we exploit it below as a pseudo-pdf (upon normalization):

$$\bar{G}(\alpha, \tau) = \frac{\exp \left\{ \rho_1 \sum_{q=1}^{\bar{Q}} I(\alpha_q, \tau_q) \right\}}{\int \cdots \int \exp \left\{ \rho_1 \sum_{q=1}^{\bar{Q}} I(\alpha'_q, \tau'_q) \right\} d\alpha' d\tau'}. \quad (23)$$

Note here that the factor  $\frac{1}{PE_s}$  involved in (21) is absorbed within the new design parameter,  $\rho_1$ . Interestingly, due to the linear decomposition in (21),  $\bar{G}(\alpha, \tau)$  is found to be *separable* in terms of the angle-delay pairs as originally required. Indeed, it can be easily shown that  $\bar{G}(\alpha, \tau)$  factorizes as follows:

$$\bar{G}(\alpha, \tau) = \prod_{q=1}^{\bar{Q}} \bar{g}_{\bar{\alpha}, \bar{\tau}}(\alpha_q, \tau_q), \quad (24)$$

where

$$\bar{g}_{\bar{\alpha}, \bar{\tau}}(\alpha, \tau) = \frac{e^{\rho_1 I(\alpha, \tau)}}{\iint e^{\rho_1 I(\alpha', \tau')} d\alpha' d\tau'}. \quad (25)$$

This simply means, under this particular choice for  $\bar{G}(\alpha, \tau)$ , that the  $\bar{Q}$  angle-delay pairs,  $\{(\alpha_q, \tau_q)\}_{q=1}^{\bar{Q}}$ , are independent and identically distributed (iid) [i.e., with common bivariate distribution  $\bar{g}_{\bar{\alpha}, \bar{\tau}}(\alpha, \tau)$ ]. from which the marginal pdf of the delays is computed as follows:

$$\bar{g}_{\bar{\tau}}(\tau) = \int \bar{g}_{\bar{\alpha}, \bar{\tau}}(\alpha, \tau) d\alpha. \quad (26)$$

#### IV. ESTIMATING THE NUMBER OF PATHS

As mentioned earlier, all the existing JADE techniques require the *a priori* knowledge of the number of paths  $\bar{Q}$ . In practice, this parameter is unknown and needs to be estimated before proceeding to AoAs and TDs acquisition. In this contribution, we propose a new heuristic approach that allows the exact estimation of  $\bar{Q}$  over a wide range of practical SNRs. In fact, it relies on a sparsity feature inherent to the marginal delay pdf,  $\bar{g}_{\bar{\tau}}(\tau)$ , depicted in Fig. 2. Indeed, by properly

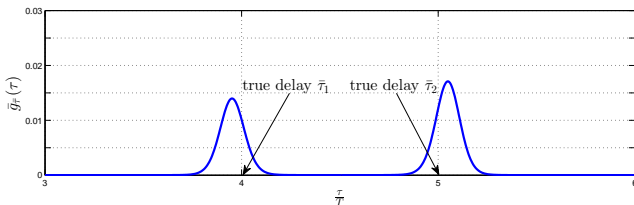


Figure 2. Marginal pdf of  $\tau$ , illustrated in a single-carrier system, ULA,  $P = 5$ ,  $\bar{Q} = 2$  and SNR = 30 dB.

selecting the *sparsity-promoting* design parameter  $\rho_1$ , it is possible to reduce the sizes of the secondary lobes that are due to the noise contribution. In this way, one obtains a pseudo-pdf whose energy is almost totally concentrated under the main lobes that are located around the true delays. Precisely, just after evaluating  $\bar{g}_{\bar{\tau}}(\tau_i)$  in (26) over  $[0, \tau_{\max}]$ , the following two simple steps are performed:

- 1) STEP 1: Get the points,  $\{\hat{\tau}_q^{\circ}\}_q^{Q_{\text{tot}}}$ , corresponding to all the peaks in  $\{\bar{g}_{\bar{\tau}}(\tau_i) \forall \tau_i \in [0, \tau_{\max}]\}$  with  $Q_{\text{tot}}$  being the total number of peaks. Note here that  $Q_{\text{tot}}$  is always greater than  $\bar{Q}$  due to the presence of secondary lobes.
- 2) STEP 2: Sort the squared magnitudes,  $\{|\bar{g}_{\bar{\tau}}(\hat{\tau}_q^{\circ})|^2\}_q^{Q_{\text{tot}}}$ , corresponding to  $\{\hat{\tau}_q^{\circ}\}_q^{Q_{\text{tot}}}$  and obtain an estimate,  $\hat{Q}$  (for the actual number of paths) as the first number of peaks,  $Q$ , whose combined energy fractions is above a certain threshold, i.e.:

$$\rho(Q) = \frac{\sum_q^Q |\bar{g}_{\bar{\tau}}(\hat{\tau}_q^{\circ})|^2}{\sum_q^{Q_{\text{tot}}} |\bar{g}_{\bar{\tau}}(\hat{\tau}_q^{\circ})|^2} \geq \kappa, \quad (27)$$

$$\rho(Q-1) = \frac{\sum_q^{Q-1} |\bar{g}_{\bar{\tau}}(\hat{\tau}_q^{\circ})|^2}{\sum_q^{Q_{\text{tot}}} |\bar{g}_{\bar{\tau}}(\hat{\tau}_q^{\circ})|^2} < \kappa, \quad (28)$$

where  $\kappa$  is some threshold level to be designed offline as explained subsequently.

As mentioned above, the threshold level,  $\kappa$ , can be easily optimized offline in order to obtain the lowest possible  $\bar{Q}$ -estimation error for all the practical values of  $\bar{Q}$ . To do so, for each  $\bar{Q}$ , the mean value of the ratio in (27), is denoted here as:

$$\bar{\rho}(Q) \triangleq \mathbb{E} \{ \rho(Q) \}, \quad (29)$$

is evaluated by Monte-Carlo simulations for all  $1 \leq Q \leq Q_{\text{tot}}$ . Then, the appropriate value for  $\kappa$  is selected based on these mean values as suggested by Fig. 3 (note here that Fig. 3(b) depicts a zoom of Fig. 3(a) around the specified region along the  $y$ -axis). These results are obtained from 10000 Monte-Carlo runs for every  $\bar{Q}$  while assuming equi-powered paths at an SNR = -10 dB.

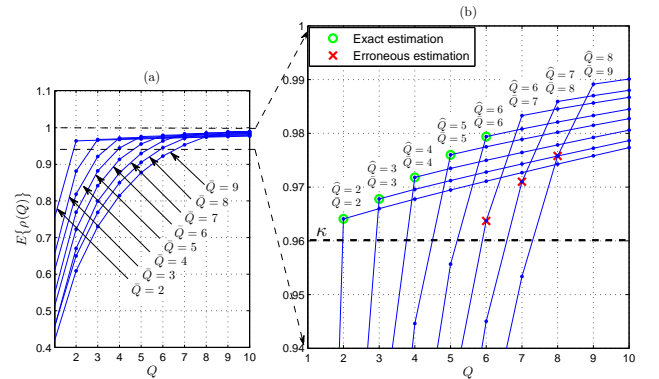


Figure 3. The mean value of  $\rho(Q)$  for different values of  $\bar{Q}$ , SNR = -10 dB.

At such extremely low SNR level, and as suggested by Fig. 3(b), an appropriate choice for the threshold level would be

$\kappa = 0.96$ . In fact, with such threshold, it is seen for  $\bar{Q} = 2$  that the first value  $Q$  at which  $\rho(Q)$  exceeds  $\kappa = 0.96$  (on average) is  $Q = 2$ , i.e., “exact estimation”. The same observation holds for  $\bar{Q} = 3, 4, 5$  and  $6$  as seen from Fig. 3(b). For  $\bar{Q} = 7$ , however, the first value  $Q$  that verifies (27) and (28) on average is  $Q = 6$ , i.e., “under-estimation” and the same observation holds as well for  $\bar{Q} = 8$  and  $\bar{Q} = 9$ .

## V. SIMULATION RESULTS

In this section, we assess the performance of the new by plotting the error probability on detecting the number of paths. The number of receiving antenna elements is fixed to  $P = 5$  and the number of samples is set to  $M = 245$ . The design parameter,  $\rho_1$ , required by our new algorithm is set to  $\rho_1 = 4$ .

In Fig. 4, we gauge our proposed approach for estimating the number of paths,  $\bar{Q}$ , against the two widely used signal detection schemes, namely MDL and AIC [11]. There, it is seen that the proposed approach outperforms both benchmarks in terms of the probability of detection error. This is mainly due to the use of the sparsity-promoting design parameter,  $\rho_1$ , whose appropriate selection allows to reduce the contributions of the spurious lobes stemming from the background noise. We emphasize, however, the fact that both MDL and AIC are

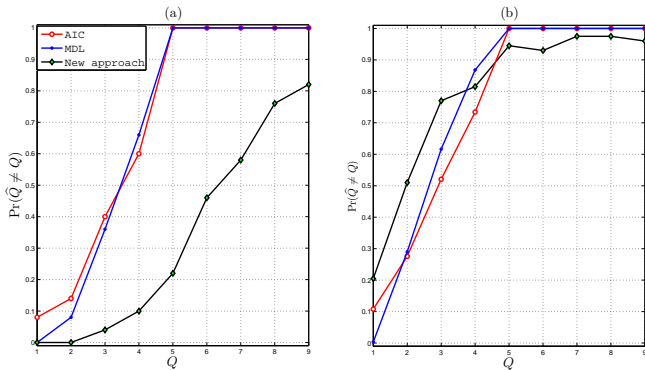


Figure 4. Error Probability on detecting the number of paths for a single-carrier system employing  $M = 245$  samples at  $\text{SNR} = 0$  dB with  $P = 5$  and  $\rho_1 = 4$ : (a) equi-powered paths and (b) paths with power generated randomly.

applicable only when the actual number of paths,  $\bar{Q}$ , is smaller than the number of receiving antenna elements  $P$  since their cost functions can be evaluated for  $1 \leq Q \leq P$  only. In contrast, the proposed approach takes advantage of the spatio-temporal model to detect all the involved paths even when  $P < Q$  shown earlier by Van der Veen *et al.* in [6] as apposed to both MDL and AIC which were both developed for the case of DOA-only estimation. This clearly observed from Fig. 4, as our technique succeeds in detecting all the  $Q$  paths for  $Q = 7, 8, 9$  using only  $P = 5$  antenna elements, contrarily to both MDL and AIC. Clearly, other JADE techniques such as TST-MUSIC or the initialisation step of the SAGE algorithm are good candidates for paths detection even when  $P < Q$ . Unfortunately those techniques have no control on the noise component. Indeed, those techniques cannot define a threshold between the pics related to the true paths and those linked

to the noise component since the latter changes from one realisation to another.

## VI. CONCLUSION

In this paper, we proposed a new path detection technique. By exploiting the sparsity feature of a pseudo-pdf, the new approach is able to accurately estimate the number of paths over a wide range of practical SNRs. Computer simulation results show the clear superiority of the new technique over state-of-the-art approaches especially when the number paths exceeds the size of the antenna array.

## REFERENCES

- [1] F. Bellili, S. Ben Amor, S. Affes, and A. Ghayeb, “Maximum Likelihood Joint Angle and Delay Estimation from Multipath and Multicarrier Transmissions with Application to Indoor Localization Over IEEE 802.11ac Radio”, *IEEE Trans. Mobile Computing*, appeared online, July 2018.
- [2] A. J. Van der Veen, “Algebraic methods for deterministic blind beamforming”, *Proc. IEEE*, vol. 86, no. 10, pp. 1987-2008, Oct. 1998.
- [3] J. T. Chen and Y. C. Wang, “Performance analysis of the parametric channel estimators for MLSE equalization in multipath channels with AWGN”, *IEEE Trans. Commun.*, vol. 49, no. 3, pp. 393-396, Mar. 2001.
- [4] F. Bellili, S. Ben Amor, S. Affes, and A. Samet, “A new importance-sampling ML estimator of time delays and angles of arrival in multipath environments”, in *Proc. of IEEE ICASSP*, pp. 4219-4223, 2014.
- [5] Y. Wang, J. Chen, and W. Fang, “TST-MUSIC for joint DOA-delay estimation”, *IEEE Trans. Sig. Process.*, vol. 49, no. 4, pp. 721-729, Apr. 2001.
- [6] M. Vanderveen, A. Vanderveen, and A. Paulraj, “Joint angle and delay estimation using shift-invariance techniques”, *IEEE Trans. Sig. Process.*, vol. 46, no. 2, pp. 405-418, Feb. 1998.
- [7] M. Wax and A. Leshem, “Joint estimation of time delays and directions of arrival of multiple reflections of a known signal”, *IEEE Trans. Sig. Process.*, vol. 45, no. 10, pp. 2477-2477, Oct. 1997.
- [8] B. H. Fleury, M. Tschudin, R. Heddergott, D. Dahlhaus, and I. K. Pedersen, “Channel parameter estimation in mobile radio environments using the sage algorithm”, *IEEE J. Sel. Areas Commun.*, vol. 17, no.3, pp. 434-450, Mar. 1999.
- [9] H. Akaike, “A new look at the statistical mode! identification,” *IEEE Trans. Automat. Contr.*, vol. AC-19, no. 6, pp. 716-723, Dec. 1974.
- [10] J. Rissanen, “Modeling by shortest data description,” *Automatica*, vol. 14, pp. 465-471, 1978.
- [11] M. WAX, and T. KAILATH, “Detection of Signals by Information Theoretic Criteria,” *IEEE Trans. Acoust., Speech and Sig. Process.*, vol. ASSP-33, No. 2, pp. 387-392, Apr. 1985.
- [12] P. Stoica and A. Nehorai, “On the concentrated stochastic likelihood function in array signal processing,” *Circuits, Syst., Signal Process.*, vol. 14, pp. 669-674, Sep. 1995.